Available online at www.sciencedirect.com
ScienceDirect
European Journal of Medicinal Chemistry 43 (2008) 996–1007
EUROPEAN JOURNAL OF MEDICINAL CHEMISTRY
http://www.elsevier.com/locate/ejmech

Original article

Inhibition of immune complex-mediated neutrophil oxidative metabolism: A pharmacophore model for 3-phenylcoumarin derivatives using GRIND-based 3D-QSAR and 2D-QSAR procedures

Luciana M. Kabeya [a], Carlos H.T.P. da Silva [b,*], Alexandre Kanashiro [a], Joaquín M. Campos [c], Ana Elisa C.S. Azzolini [a], Ana Cristina M. Polizello [a], Mônica T. Pupo [b], Yara M. Lucisano-Valim [a,**]

[a] *Departamento de Física e Química, Faculdade de Ciências Farmacêuticas de Ribeirão Preto da Universidade de São Paulo. Av. Café s/n, Bairro Monte Alegre, Ribeirão Preto, SP, CEP 14040-903, Brazil*
[b] *Departamento de Ciências Farmacêuticas, Faculdade de Ciências Farmacêuticas de Ribeirão Preto da Universidade de São Paulo. Av. Café s/n, Bairro Monte Alegre, Ribeirão Preto, SP, CEP 14040-903, Brazil*
[c] *Departamento de Química Farmacéutica y Orgánica, Facultad de Farmacia, Campus de Cartuja s/n, 18071 Granada, Spain*

Received 16 April 2007; received in revised form 27 June 2007; accepted 2 July 2007
Available online 15 July 2007

Abstract

In this study, twenty hydroxylated and acetoxylated 3-phenylcoumarin derivatives were evaluated as inhibitors of immune complex-stimulated neutrophil oxidative metabolism and possible modulators of the inflammatory tissue damage found in type III hypersensitivity reactions. By using lucigenin- and luminol-enhanced chemiluminescence assays (CL-luc and CL-lum, respectively), we found that the 6,7-dihydroxylated and 6,7-diacetoxylated 3-phenylcoumarin derivatives were the most effective inhibitors. Different structural features of the other compounds determined CL-luc and/or CL-lum inhibition. The 2D-QSAR analysis suggested the importance of hydrophobic contributions to explain these effects. In addition, a statistically significant 3D-QSAR model built applying GRIND descriptors allowed us to propose a virtual receptor site considering pharmacophoric regions and mutual distances. Furthermore, the 3-phenylcoumarins studied were not toxic to neutrophils under the assessed conditions.

Keywords: Coumarin; 2D-QSAR; 3D-QSAR; Immune complexes; Neutrophil; GRIND

1. Introduction

Formation and clearance of circulating antigen–antibody complexes or immune complexes (ICs) are essential processes in humoral immune defense mechanisms [1]. Deposition of ICs within tissues triggers an inflammatory reaction called type III hypersensitivity characterized by large neutrophil infiltration. This process has been found in diseases such as systemic lupus erythematosus, rheumatoid arthritis and autoimmune vasculitis [2]. Phagocytosis and degranulation, and the oxidative metabolism, which produces reactive oxygen species (ROS) are effector functions triggered by IC-activated neutrophils. These functions are involved in ICs' digestion, microbial killing and regulation of the inflammatory process. However, activated neutrophils also release large amounts of enzymes and ROS to the extracellular milieu overpowering the local antioxidant defense systems and contributing to tissue damage and the amplification of the inflammatory process [1–4].

* Corresponding author. Tel.: +55 16 36024717; fax: +55 16 36024879.
** Corresponding author. Tel.: +55 16 36024434; fax: +55 16 36024880.
E-mail addresses: tomich@fcfrp.usp.br (C.H.T.P. da Silva), yaluva@usp.br (Y.M. Lucisano-Valim).

0223-5234/$ - see front matter © 2007 Elsevier Masson SAS. All rights reserved.
doi:10.1016/j.ejmech.2007.07.003

The involvement of neutrophil-derived ROS in the physiopathology of many inflammatory diseases has been attracting interest in the discovery of new compounds with antioxidant and immunomodulatory properties, which might supplement the endogenous antioxidant defense system and modulate the neutrophil respiratory burst [5]. In this context, our research group has been investigating the biological activities of plant secondary metabolites such as coumarins, flavonoids and sesquiterpene lactones and studying their structure–activity relationships [6–8]. The importance of free hydroxyl groups for the antioxidant activity in cell-free experimental models has been highlighted by our data, in agreement with the literature [9–12]. However, in cell-mediated oxidative and inflammatory processes, esterification of hydroxyl groups in phenolic compounds has also been reported as an important structural feature that increases their immunomodulatory properties [6,13,14].

Phenylcoumarins constitute a class of plant secondary metabolites produced by the same biosynthetic pathway of flavonoids and are also characterized by a C6–C3–C6 chain [15,16]. Few reports indicate biological activities of this class of compounds such as antifungal and antibacterial [17]. Recently, our research group reported the action of some phenylcoumarin derivatives as antioxidants and inhibitors of glyceraldehyde-3-phosphate dehydrogenase from *Trypanosoma cruzi* and horseradish peroxidase [18,19]. However, the biological effects of these compounds on cells in the immune system are still not well known.

In the present study, we investigated the modulatory effects of a series of hydroxylated and acetoxylated 3-phenylcoumarin derivatives on the IC-mediated neutrophil oxidative metabolism, as well as their toxic effect on these cells. Moreover, the qualitative structure–activity relationships were discussed and the quantitative aspects were analyzed by 2D- and 3D-QSAR approaches.

2. Results and discussion

2.1. Inhibition of immune complex-mediated neutrophil oxidative metabolism

Low-molecular-weight natural coumarins and their synthetic derivatives are a novel class of potential anti-inflammatory drugs studied with great interest [20,21]. Kontogiorgis and Hadjipavlou-Litina [22] recently demonstrated a high anti-inflammatory effect of coumarin derivatives on carrageenan-induced paw edema and adjuvant-induced arthritis in rat models. The authors suggested that this activity might be associated with the inhibition of cyclooxygenase and lipoxygenase pathways and/or to the antioxidant behaviour of the compounds. In a previous study, our research group reported the inhibitory effect of simple coumarins on neutrophil superoxide anion generation [6].

In this investigation, the modulatory effects of new hydroxylated and acetoxylated 3-phenylcoumarin derivatives, synthesized as previously described [18,19] (Fig. 1) were evaluated on the IC-mediated neutrophil oxidative metabolism. In order to gain an initial insight as to which steps of the respiratory burst activation might be affected by the tested compounds, two different chemiluminescent probes, luminol and lucigenin were used. The production of superoxide anion, the first ROS generated by the NADPH enzymatic complex can be specifically measured by lucigenin. The other ROS produced in subsequent steps, especially those involved in the myeloperoxidase-hydrogen peroxide-Cl^- reaction, can be measured by luminol [23].

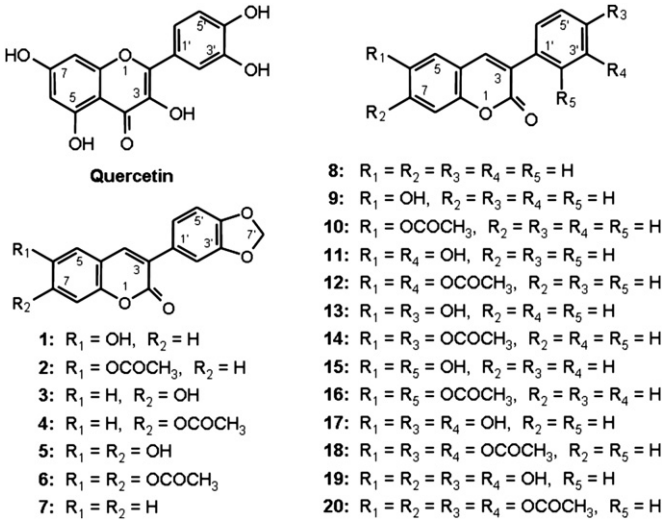

Fig. 1. Chemical structures of quercetin and 3-phenylcoumarin derivatives.

The inhibitory effect of 3-phenylcoumarins on the neutrophil respiratory burst was first screened at 50 μM (Table 1). Non-substituted 3-phenylcoumarins **7** and **8** did not show a significant inhibitory effect on either lucigenin- or luminol-enhanced chemiluminescence (CL-luc or CL-lum, respectively), whereas compounds **1–4**, **9** and **11** inhibited CL-luc but not CL-lum, under the assessed conditions. The active compounds showed concentration-dependent inhibitory effects on the neutrophil function when evaluated in six concentrations (0–50 μM) (data not shown). IC_{50} values are reported in Table 1.

Hydroxylated (**5**) and acetoxylated derivatives **6** and **20** were the most effective inhibitors of the two steps of the neutrophil respiratory burst investigated. Their IC_{50} values in the CL-luc and CL-lum assays were significantly lower than the ones for the standard compound quercetin, a widely known inhibitor of neutrophil effector functions [5]. The inhibitory potency of the other compounds was similar to or lower than that of quercetin. Moreover, the structural features contributing to inhibition of CL-luc and/or CL-lum were quite different in the set of 3-phenylcoumarin derivatives here investigated.

Regarding CL-luc, which measures $O_2^{\bullet -}$ generation, it was observed that only non-substituted 3-phenylcoumarins **7** and **8** were not inhibitory at 50 μM, suggesting that the presence of hydroxyl or acetoxyl groups is essential for this biological activity. Increasing the number of total hydroxyl groups in the molecule did not promote a significant enhancement of inhibitory activity (**9**, **11**, **13**, **15**, **17**, **19**), except when associated

Table 1
Inhibitory effects of 3-phenylcoumarins on the immune complex-stimulated neutrophil oxidative metabolism

Compound[a]	Inhibition at 50 μM[b] (%)		IC_{50}[b] (μM)	
	CL-luc[c]	CL-lum[d]	CL-luc	CL-lum
1	83.5 ± 6.5	23.2 ± 1.5	5.6 ± 1.7	>50
2	68.0 ± 0.6	13.7 ± 8.8	5.4 ± 1.6	>50
3	79.4 ± 1.6	17.5 ± 6.8	8.6 ± 1.8**	>50
4	67.1 ± 8.9	7.9 ± 6.9	7.3 ± 3.5*	>50
5	99.6 ± 0.1	99.8 ± 0.1	0.7 ± 0.1**	0.7 ± 0.2*
6	99.0 ± 0.3	99.4 ± 0.1	0.7 ± 0.2**	0.7 ± 0.1*
7	5.7 ± 4.0	10.1 ± 3.4	>50	>50
8	27.9 ± 5.4	9.0 ± 6.0	>50	>50
9	83.5 ± 1.3	21.8 ± 5.1	8.0 ± 2.6**	>50
10	80.5 ± 0.6	50.5 ± 0.2	7.4 ± 2.3*	31.2 ± 5.2**
11	94.1 ± 0.9	31.7 ± 5.4	5.2 ± 1.1	>50
12	82.1 ± 0.1	66.3 ± 2.1	6.9 ± 1.6	21.7 ± 4.2**
13	95.7 ± 0.4	69.8 ± 0.6	4.3 ± 1.0	29.6 ± 7.7**
14	92.5 ± 0.6	60.3 ± 4.0	4.0 ± 0.5	27.4 ± 5.0**
15	99.9 ± 0.1	99.0 ± 0.1	2.5 ± 0.5	2.8 ± 0.2
16	96.5 ± 0.1	94.6 ± 0.1	2.6 ± 0.4	2.9 ± 0.3
17	98.7 ± 0.6	99.2 ± 0.1	4.4 ± 0.7	4.9 ± 0.5
18	97.5 ± 0.3	92.3 ± 0.1	1.8 ± 0.1*	2.0 ± 0.2
19	94.9 ± 0.9	92.4 ± 1.6	5.2 ± 1.6	13.4 ± 1.3**
20	99.9 ± 0.1	99.9 ± 0.1	0.4 ± 0.1**	0.4 ± 0.1*
Quercetin	99.9 ± 0.1	99.9 ± 0.1	4.7 ± 0.8	2.4 ± 0.7

Statistics: $p < 0.05$(*) and $p < 0.01$ (**) vs. quercetin (ANOVA and Dunnett's *post-hoc* test).

[a] Chemical structures shown in Fig. 1.

[b] Data are means ± standard deviation of three independent experiments with duplicate measurements.

[c] CL-luc: lucigenin-enhanced chemiluminescence.

[d] CL-lum: luminol-enhanced chemiluminescence.

with the methylenedioxyl group (**1**, **3**, **5**). On the other hand, the inhibitory activity increased with the number of acetoxyl groups, and the presence of vicinal acetoxyl groups (**6**, **18**, **20**) were also relevant to CL-luc inhibition by this set of compounds. Furthermore, acetylation of the hydroxyl groups of the mono or dihydroxylated 3-phenylcoumarins (**1**, **3**, **5**, **9**, **11**, **13**, **15** vs. **2**, **4**, **6**, **10**, **12**, **14**, **16**) did not have a significant effect on the inhibitory activity of the compounds, but increased the inhibitory potency of the tri and tetrahydroxylated compounds (**17**, **19** vs. **18**, **20**).

With regard to CL-lum, which measures the overall ROS production by the activated neutrophils (mainly those involved in the myeloperoxidase-catalyzed reaction), it was observed that compounds bearing the 3′,4′-methylenedioxyl group and a free or esterified hydroxyl group at C-6 or C-7 (**1**–**4**) had no significant inhibitory effect in the highest concentration tested, but 3-phenylcoumarins bearing a 6,7-dihydroxyl or 6,7-diacetoxyl group (**5**, **6**) had quercetin-similar inhibitory effects. Moreover, the presence of a hydroxyl group at C-2′ or the 3′,4′-dihydroxyl group (**15**, **17**) in the 6-hydroxylated compounds led to a significant inhibition of CL-lum when compared to other positions; however, the increase in the total number of hydroxyl groups, i.e. 6,7,3′,4′-tetrahydroxylation, significantly reduced the inhibitory potency (**17** vs. **19**). Considering the 6-acetoxylated compounds, additional acetoxyl groups at C-2′ or C-3′, as well as the 3′,4′-diacetoxyl group in compounds (**12**, **16**, **18**) increased the inhibitory effect on CL-lum when compared to other positions. On the other hand, esterification of hydroxyl groups did not influence the inhibitory activity of 3-phenylcoumarins bearing one, two or three substituents but significantly increased the inhibitory effect of the tetrahydroxylated compound (**19** vs. **20**).

In summary, compounds with similar IC_{50} values for CL-luc and CL-lum had the following structural features: (a) one or two *ortho*-diacetoxyl groups (**6**, **18**, **20**); (b) *ortho*-dihydroxyl groups (**5**, **17**); (c) hydroxyl or acetoxyl groups on C-6 and C-2′ (**15**, **16**). These features suggest that the compounds act on biochemical pathways shared by the $O_2^{\bullet -}$ and other ROS generation, such as IC recognition by the Fcγ receptor on the neutrophil membrane and activation of protein kinases. Ursini et al. [24] demonstrated that flavonoids, another polyphenolic class with known antioxidant and immunomodulatory properties, could also act as unspecific inhibitors of several kinds of protein kinases.

The structural features of 3-phenylcoumarins that inhibited CL-luc more than CL-lum were: (a) a single hydroxyl or acetoxyl group at C-6 or C-7 (**1**–**4**, **9**, **10**); (b) two hydroxyl or acetoxyl groups, one placed at C-6 and the other at C-3′ or C-4′ (**11**–**14**); (c) two *ortho*-dihydroxyl groups (**19**). The mechanisms involved in this highly inhibitory effect on CL-luc when compared to CL-lum seem to be related to a selective action of these 3-phenylcoumarin derivatives on $O_2^{\bullet -}$ generating pathways. This possibility will be assessed in a further study.

Payá et al. [25,26] reported that the presence of *ortho*-dihydroxyl groups increased the free radical scavenger and inhibitory effects of simple coumarins on human and rat neutrophil oxidative metabolism. The results of the present study are in partial agreement with this observation, since the 6,7-dihydroxylated 3-phenylcoumarin derivative **5** was one of the most effective inhibitors of neutrophil oxidative burst. However, an additional *ortho*-dihydroxyl group in the 3-phenyl ring (**19**) reduced the inhibitory potency on this cellular function. In addition, the other two 3-phenylcoumarins inhibiting CL-luc and CL-lum more than quercetin were the acetoxylated derivatives **6** and **20**, where the hydroxyl groups were acetylated. Interestingly, substitution of the 3′,4′-dihydroxyl groups by 3′,4′-methylenedioxyl did not influence the inhibitory potency of the 6-hydroxylated compound (**17** vs. **1**) on CL-luc but decreased its inhibitory effect on CL-lum. This structural modification also increased the inhibitory effect of the 6,7-dihydroxylated compound (**19** vs. **5**) on both, CL-luc and CL-lum. However, substitution of the 3′,4′-diacetoxyl group by 3′,4′-methylenedioxyl reduced the inhibitory effect of the 3-phenylcoumarin bearing a 6-acetoxyl group (**18** vs. **2**, $p < 0.01$) but did not influence the inhibitory effect of the 6,7-diacetoxylated compound (**20** vs. **6**) on both CL-luc and CL-lum. Together, these results suggest that other factors besides the presence of free hydroxyl groups are involved in the inhibition of neutrophil oxidative metabolism by the 3-phenylcoumarins tested herein.

The cytotoxic effect of the 3-phenylcoumarin derivatives on neutrophils was also evaluated, since this could be one of the mechanisms underlying inhibition of cellular oxidative metabolism and chemiluminescence production [23]. The

compounds tested in final concentrations of 50 μM did not induce significant lactate dehydrogenase release or decrease in cellular viability when compared to the controls (Table 2) indicating that they were not toxic to the neutrophils under the conditions assessed.

2.2. 3D-QSAR studies

In the present investigation, the inhibitory effects of the 3-phenylcoumarin derivatives on the IC-mediated neutrophil oxidative metabolism were investigated by using both luminol- and lucigenin-dependent chemiluminescence assays (CL-lum and CL-luc, respectively). In order to analyze a possible relationship between the activities of the compounds here investigated and their structures, we focused on a series of 13 structures (**5**, **6**, **10**, **12**–**20** and quercetin) that showed measurable IC_{50} values for the CL-lum (Table 1). A 3D-QSAR model using 18 compounds with measurable IC_{50} values for the CL-luc was also built but it did not survive the cross-validation; therefore, it was not considered in this study.

First, suitable 3D structures were obtained for these compounds using molecular mechanics and Hartree-Fock/Density Functional Theory, as detailed in the Section 4. In the 3D-QSAR model, biological activity of the compounds has been indicated by pIC_{50} values. Using this 3D-QSAR approach, the model can be obtained without the need of a 3D-alignment of the structures [27]. In a few words, GRIND starts with the calculation of molecular interaction fields (MIF) using GRID, which describes regions where the ligand can produce energetically favorable interactions with probes representing potential groups of the receptor. Subsequently, GRIND transforms (filters) a number of these MIF in a small number of variables describing the existence at a certain distance of pairs of points representing favorable or unfavorable interactions. These variables are grouped in blocks (correlograms) and their analysis allows investigation of the main interactions between the series of ligands and the receptor. Further details about the GRIND method can be found in the original reference of Pastor et al. [27]. Our results were thus interpreted in a convenient pharmacophoric-like model, allowing us to propose a virtual model of the receptor site (VRS) as well as to identify the structural groups/characteristics that were common to the most active ligands.

Table 2
Neutrophil viability after treatments with quercetin, 3-phenylcoumarin derivatives at 50 μM[a] and DMSO as control

Compound[b]	Cell viability[c] (%)	LDH release[d] (% of total)
DMSO	92.9 ± 3.4	12.4 ± 2.0
1	93.8 ± 1.9	9.0 ± 1.1
2	95.5 ± 1.9	11.4 ± 0.7
3	94.3 ± 2.6	11.1 ± 0.8
4	94.3 ± 2.5	13.8 ± 2.1
5	93.2 ± 4.5	15.3 ± 1.9
6	95.0 ± 2.6	11.9 ± 1.0
7	96.0 ± 2.0	11.9 ± 0.9
8	90.3 ± 2.2	17.1 ± 0.4
9	92.3 ± 3.2	10.7 ± 2.2
10	93.8 ± 1.0	11.3 ± 0.9
11	93.8 ± 0.5	11.2 ± 1.4
12	94.0 ± 1.8	9.3 ± 1.6
13	89.5 ± 3.9	18.3 ± 2.3
14	92.5 ± 2.4	11.6 ± 2.0
15	94.8 ± 1.5	9.8 ± 2.4
16	90.3 ± 3.3	14.6 ± 1.3
17	92.8 ± 4.0	11.9 ± 2.5
18	93.3 ± 4.1	9.3 ± 4.0
19	92.0 ± 2.2	10.5 ± 0.8
20	88.8 ± 4.9	20.7 ± 1.8
Quercetin	93.0 ± 4.0	10.9 ± 2.6

[a] Cells were treated with DMSO (dimethylsulfoxide), quercetin or the 3-phenylcoumarin derivatives during 30 min at 37 °C. Data are means ± standard deviation of three independent experiments with duplicate measurements.
[b] Chemical structures shown in Fig. 1.
[c] Determined by the Trypan Blue exclusion test, based on counts of 100 cells.
[d] Total cell lysis (100% LDH activity) was achieved with Triton X-100 (0.2% v/v), used as the positive control. LDH: lactate dehydrogenase.

In the final model, a total of 213 descriptors were derived after variable selection via FFD (fractional factorial design). Two LVs (latent variables) were found to be significant for internal validation using cross-validation, and the model explained a significant amount of variance (75.7%), and survived model validation ($r^2 = 0.95$; SDEC = 0.14; $q^2_{LOO} = 0.76$ by internal validation; SDEP = 0.32).

The PLS (partial least square) scores plot for two LVs and the experimental vs. calculated Y data plot shown in Fig. 2 prove the high statistical significance and quality of the PLS model obtained. According to Fig. 2A, PC1 (principal component 1) was able to discriminate the most and the least active compounds, while PC2 (principal component 2) discriminated hydroxylated and acetoxylated compounds. The PC1 of ALMOND descriptors is mainly affected by the hydrogen bond acceptor capabilities of the molecules, whereas the interactions with the DRY (hydrophobic) and TIP (shape) probe are related to the PC2 [28]. In the first analysis, the high inhibitory activity of some acetoxylated compounds such as **20** and **6** can be explained by a greater hydrophobicity in comparison to their corresponding hydroxylated compounds, as well as by their larger size that allow a better fit into the receptor. On the other hand, the presence of acetoxyl groups allows them to accept stronger hydrogen bonds from the receptor. In Fig. 2B, the molecules can be separated in three clusters according to their biological activity values (Y), where the right-hand side contains the most active compounds (largest pIC_{50} values).

The PLS coefficients for a model of two components were represented as a bar diagram to identify and select the variables that strongly correlated with the Y variable (Fig. 3). In this plot, a positive value of a coefficient corresponds to a direct correlation with the Y, whereas negative values indicate an inverse correlation. The same plot also pointed out the impact of the variables on Y, where large values mean a strong impact and low values mean a weak impact on the biological activity. Every peak in this plot indicates that the VRS contains two regions separated by a distance corresponding to the abscissa of the peak (short distances appear on the left-hand side and greater distances on the right-hand side). The height of the peak expresses the product of the intensity of the field on both nodes [27].

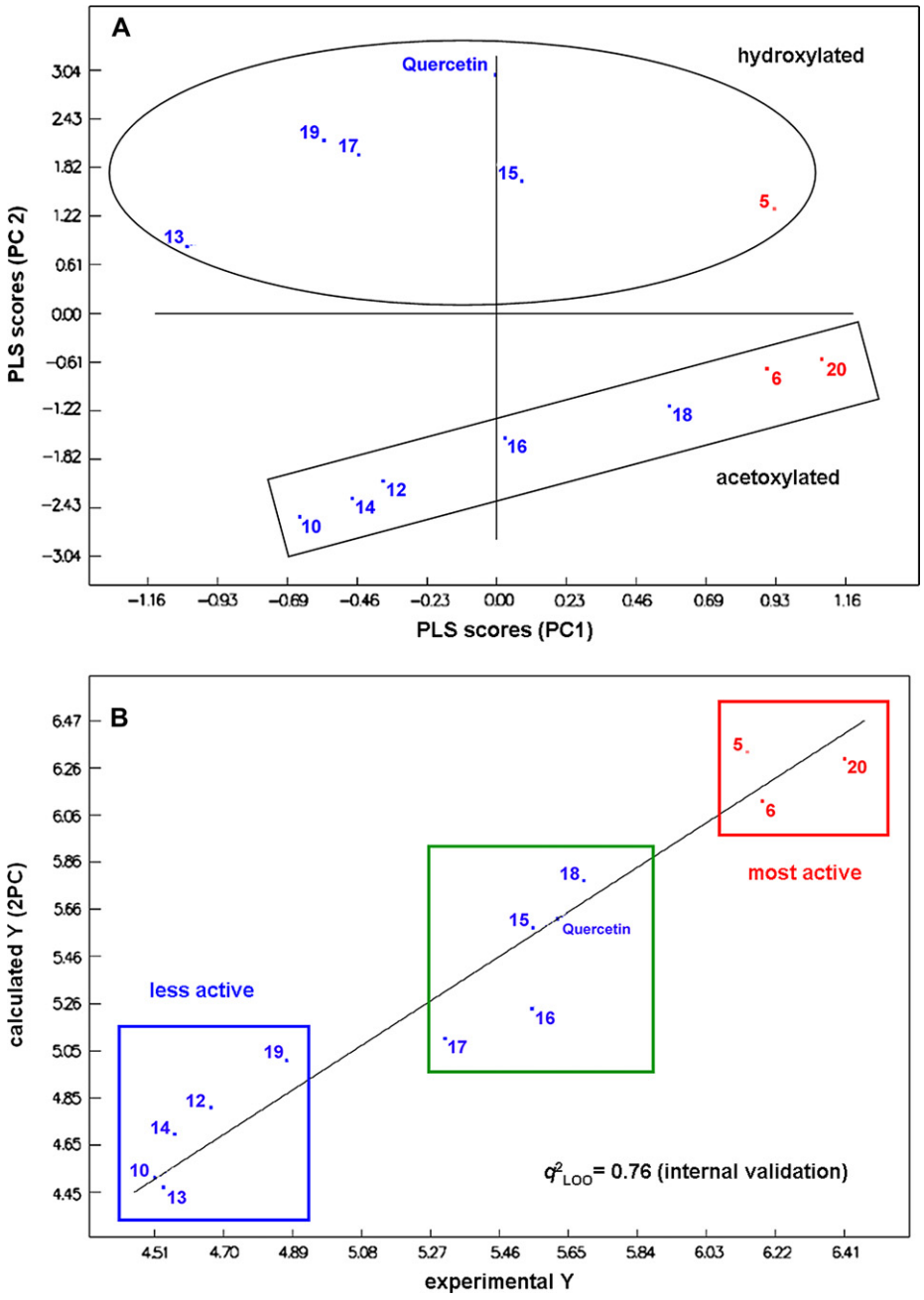

Fig. 2. In (A), the scores plot of a PLS discriminant analysis including a data set of 13 3-phenylcoumarin derivatives. PC1 is able to discriminate between the most and the least active compounds. Additionally, PC2 is able to discriminate between hydroxylated (inside the ellipse) and acetoxylated compounds (inside the rectangle). In (B), the plot of the experimental vs calculated *Y* data. Compounds are clustered regarding to their biological activity values: in red, the most active; in green, medium activity, and in blue, the less active compounds (For interpretation of the references to colour in this figure legend, the reader is referred to the web version of this article).

In Fig. 3, each block (or correlogram) of variables corresponds to a type of interaction between a couple of nodes. D (DRY) nodes indicate hydrophobic groups of the VRS, whereas O nodes indicate hydrogen bond acceptor groups, N (N1) nodes indicate hydrogen bond donor groups and T (TIP) nodes point out the shape of the virtual receptor site. Our PLS coefficients plot contains 10 correlograms derived from the four probes used, where DD, OO, NN, TT are auto-correlograms and DO, DN, DT, ON, OT and NT are cross-correlograms.

A first inspection of the coefficients plot in Fig. 3 enabled us to select some *X* variables with the highest impact on the *Y* variable. The largest peaks were related to the N1 probe (correlograms NN, NT and DN), which represent hydrogen bond donor groups of the VRS, as well as the TIP probe (correlograms NT and TT). Weak relationships with the activity were related to the O probe, suggesting that in a preliminary analysis the presence and orientation of hydrogen bond groups in this class of compounds, as well as the size and shape of the molecules were crucial for the biological activity here investigated.

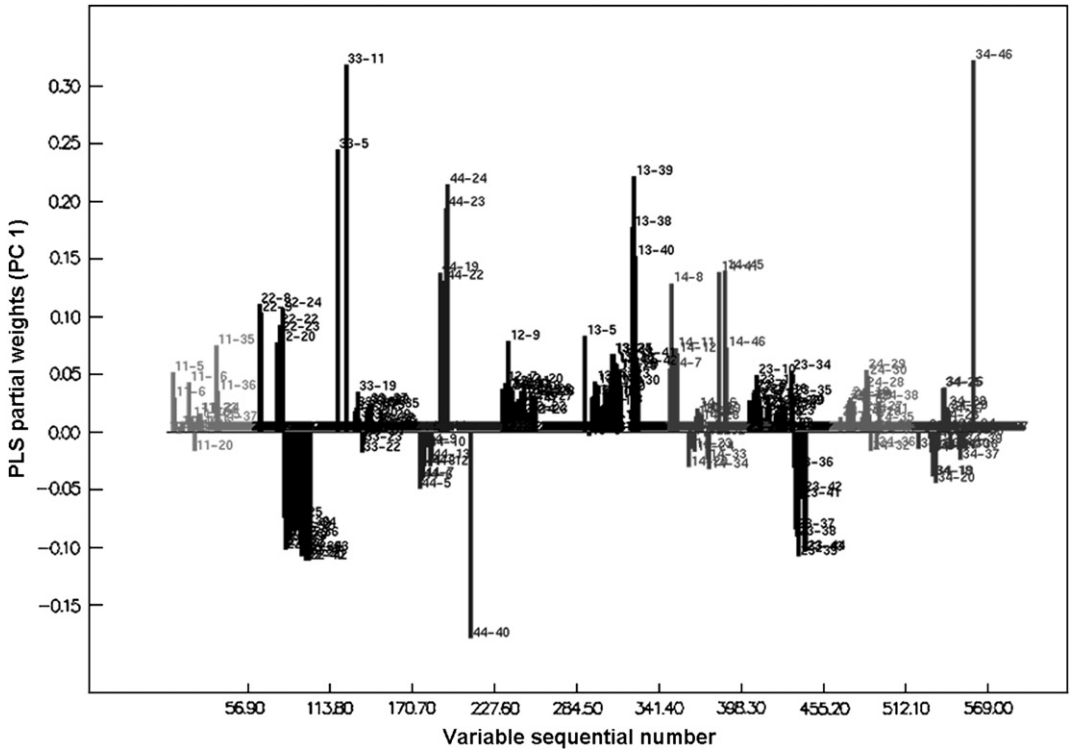

Fig. 3. PLS coefficients plot showing selected peaks corresponding to the *X* variables with the most significant impact on the biological activity (*Y*): positive values of a coefficient indicate a direct correlation to the *Y*, and negative ones indicate an inverse correlation to the *Y*, whereas large values mean a strong impact, and low values mean a weak impact.

Variable NT-46 explained the largest pIC_{50} values measured for **5**, **6** and **20** but not for **19** (Fig. 4). Our 3D-QSAR model indicated an optimum distance between N1 and TIP nodes that was crucial to the biological activity of compounds **5**, **6** and **20**. This distance (18.4 Å) was calculated from the corresponding variable sequential number (46) multiplied by the grid spacing (0.5 Å) and the smoothing window (0.8). Compound **19** was not as large as the three most active compounds above described, despite having two pairs of vicinal hydroxyl groups that could accept a hydrogen bond from the VRS. On the other hand, compounds **5**, **6** and **20** bear two vicinal carbonyl or hydroxyl groups that can accept this hydrogen bond of the VRS, and were placed at an optimum distance from the opposite extremity of the molecule. In addition, inverted orientations of **6** and **20** inside the VRS were observed after analysis of the graphical representations corresponding to the correlogram NT, and reinforced by analysis of correlograms DN and TT.

Variable DN-39 indicated a significant distance of 15.6 Å between DRY and N1 nodes that were crucial to the biological activity (Fig. 5). Regarding the VRS, it must have a hydrophobic group able to bind the benzodioxole ring of **5** and **6** in addition to the hydrogen bond donor group previously discussed. The significant distance between DRY and N1 was also found in the graphical representation of this variable for compound **20**, and was related to the distance between the methyl of the acetoxyl group of its coumarinic system and the carbonyl groups of the two acetoxyl groups present in its benzene ring. The significant distance found between the N1 node and the small DRY node (due to the interaction with the methyl of the acetoxyl group of **20** joined to the results obtained with this variable for **5** and **6**) highlighted the importance of both hydrophobic and hydrogen bond acceptor groups inversely at C-7 and C-3 position, and also indicated the ideal size of the ligand.

Variable TT-40 indicated an inverse relationship between this variable and the biological activity of the set of 3-phenylcoumarins. The negative impact on *Y* observed in the auto-correlogram TIP−TIP for this variable can be explained by an inadequate shape (i.e. an inverse orientation) of one acetoxyl group of **5**, whereas the input conformation of **20** was correct (Fig. 6). Despite the fact that GRIND is independent of the input conformations of the compounds, and hence of the 3D-alignment, this method is not insensible to the different conformers that can be used to build a 3D-QSAR model [27]. This result obtained with the variable TT-40 strongly suggests the importance of two vicinal groups capable of accepting a hydrogen bond from the receptor, reinforcing the results obtained with the variable NT-46 that pointed out the positive impact on the biological activity due to two vicinal acetoxyl or hydroxyl groups in the benzene ring of these compounds.

The auto-correlogram TIP−TIP also indicated a significant distance of 9.6 Å in the VRS due to the variable TT-24, where the strong and positive peak explained the high activity of **20** through the largest fit within the active site (Fig. 7). Although

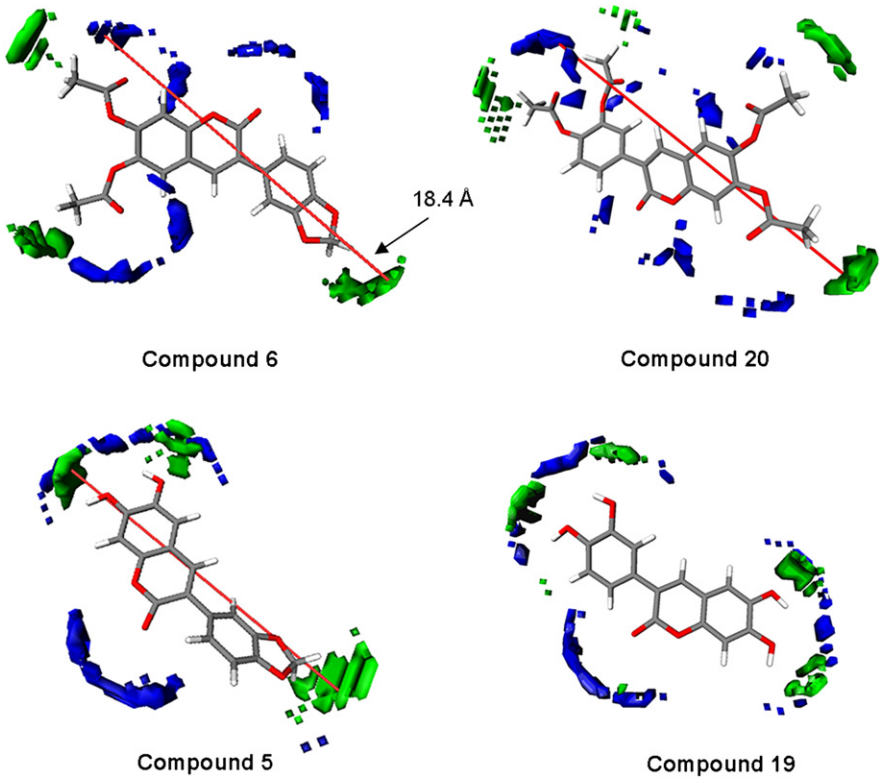

Fig. 4. Graphical display of GRIND variable 46 of the N1–TIP cross-correlogram for selected 3-phenylcoumarin derivatives. A significant distance of 18.4 Å (red line) connecting a couple of filtered nodes and corresponding to a positive impact on the biological activity was found only for the most active compounds **5**, **6** and **20** (For interpretation of the references to colour in this figure legend, the reader is referred to the web version of this article).

compound **6** did not bear groups that fit the VRS in a similar position, its high activity can be explained by the presence of a hydrophobic group (benzodioxole ring) at C-7 position (Fig. 5).

Finally, the most important descriptors in our PLS model can be arranged to obtain an approximate pharmacophore valid for the class of compounds here studied. This resulting pharmacophore, in which MIF are considered as pharmacophoric regions, consists of a hydrogen bond acceptor group and one hydrophobic group at C-7 position, and the size of the ligand also plays an important role for the ligand–receptor interaction (Fig. 8).

2.3. 2D-QSAR studies

Although sometimes taken as a criterion, prediction is not the primary goal of QSAR analyses. If it results from interpolation, it is often trivial; if extrapolation goes too far outside the included parameter space, it usually fails. QSAR helps to understand structure–activity relationships in a quantitative manner and to find the borders of certain properties.

In deriving Eqs. (1) and (2) we have used the following σ_I values: –OH: 0.29; –OAc: 0.33 [29] and the $-OCH_2O-$ grouping has been assimilated to two $-OCH_3$ groups (σ_I: 0.27) [30] in the 3′ and 4′ carbon atoms, because the σ_I value of the methylenedioxy group is unknown. The following hydrophobic substituent constants have been used for Eq. (2): –OAc: −0.64 [31]; the $-OCH_2O-$ moiety was substituted by a $-OCH_3$ group (π: −0.02) [31] at position C-3′; H– (π: 0.00), and –OH (π: −0.67) [31]. We have obtained the two following equations, where the subscripts refer to the position of the substituents:

$$\begin{aligned} p\mathrm{IC}_{50\ \text{CL-luc}} &= 4.21 + 2.92(\pm 0.66)\sigma_I R_6 + 1.94(\pm 0.52)\sigma_I R_7 \\ &\quad + 1.53(\pm 0.73)\sigma_I R_{2'} + 0.26(\pm 0.52)\sigma_I R_{3'} \\ &\quad + 0.79(\pm 0.52)\sigma_I R_{4'} \\ n = 18,\ s = 0.243,\ r^2 &= 0.745,\ F_{5,12} = 7.02,\ \alpha < 0.005 \quad (1) \end{aligned}$$

where $p\mathrm{IC}_{50} = -\log \mathrm{IC}_{50}$ of the lucigenin-dependent chemiluminescence (CL-luc), bearing in mind that the higher the value of $p\mathrm{IC}_{50}$ the more potent is the compound, n is the number of compounds, r^2 is the correlation coefficient, s is the standard deviation, data within parentheses are standard errors of estimate, and σ_I is the field-inductive substituent constant. The Fisher test (F) is highly significant here ($\alpha < 0.001$). The F value indicates the probability that the equation is a true relationship between the results, or merely coincidence. If the experimental figure exceeds the limiting value, the relationship is a true one, within the given probability level. Consultation of a table for 0.005 points [32] of the F distribution gives $F_{5,12} = 6.07$ ($\alpha < 0.005$); therefore, the probability of Eq. (1) representing an aleatory relationship is lower than

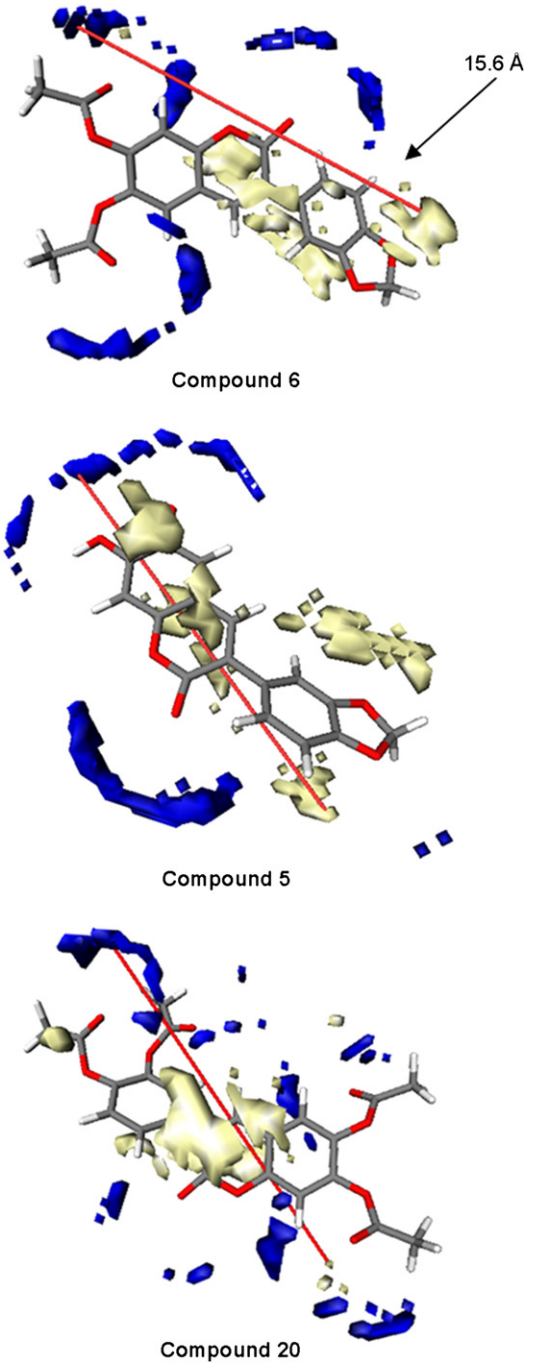

Fig. 5. Graphical display of GRIND variable 39 of the DRY–N1 cross-correlogram for selected 3-phenylcoumarin derivatives. A significant distance of 15.6 Å (red line) connecting a couple of filtered nodes and corresponding to a positive impact on the biological activity was found for the most active compounds **5**, **6** and **20** (For interpretation of the references to colour in this figure legend, the reader is referred to the web version of this article).

1 in 200 and higher than 199 in 200, indicating that the results obtained are truly related in the manner given. As can be seen in Eq. (1) the term $\sigma_I R_{3'}$ was not reliable because its standard error is higher than its coefficient. We then decided to investigate if the influence of the $R_{3'}$ was hydrophobic and Eq. (2) was obtained:

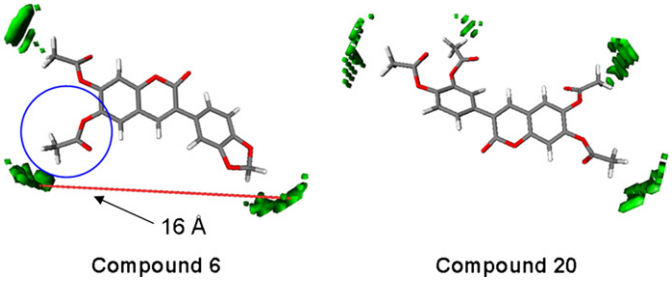

Fig. 6. Graphical display of GRIND variable 40 of the TIP–TIP auto-correlogram for the two most active 3-phenylcoumarin derivatives. A significant distance of 16 Å (red line) connecting a couple of filtered nodes and corresponding to a negative impact on the biological activity was found for the second most active compound (**6**), suggesting an inadequate shape for its acetoxyl group (inside the blue circle) in the conformation input (For interpretation of the references to colour in this figure legend, the reader is referred to the web version of this article).

$$pIC_{50\ \text{CL-luc}} = 4.26 + 2.79(\pm 0.51)\sigma_I R_6 + 1.96(\pm 0.51)\sigma_I R_7 + 1.50(\pm 0.70)\sigma_I R_{2'} + 0.16(\pm 0.31)\pi^2 R_{3'} + 0.84(\pm 0.52)\sigma_I R_{4'}$$
$$n = 18,\ s = 0.242,\ r^2 = 0.746,\ F_{5,12} = 7.05,\ \alpha < 0.005 \quad (2)$$

where π is the substituent hydrophobic constant.

The Fisher tests for Eqs. (1) and (2) were significant ($\alpha < 0.005$). The quality of the two Eqs. (1) and (2) was almost identical. Nevertheless, Eq. (2) was preferred since it has a slightly better standard deviation than Eq. (1). The significance of π in QSAR equations of some ligand-enzyme interactions has being interpreted with the help of 3D structures. These investigations showed that substituents modelled by π bind in a hydrophobic space [33,34].

Eqs. (1) and (2) are referred to CL-luc. The values of compounds **7** and **8** were not included because their pIC_{50} values

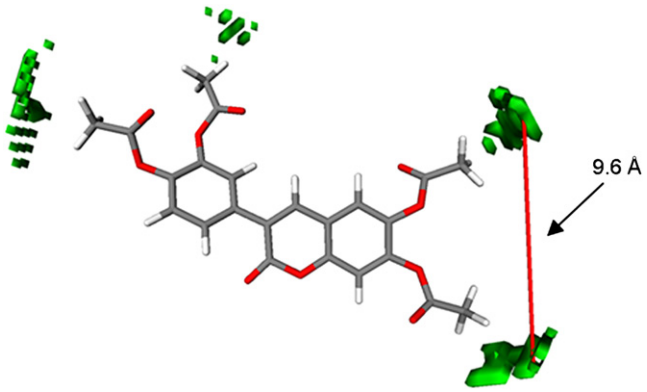

Fig. 7. Graphical display of GRIND variable 24 of the TIP–TIP auto-correlogram for the two most active 3-phenylcoumarin derivatives. A significant distance of 9.6 Å (red line) connecting a couple of filtered nodes and corresponding to a positive impact on the biological activity was found for **20** but not for **6** (For interpretation of the references to colour in this figure legend, the reader is referred to the web version of this article).

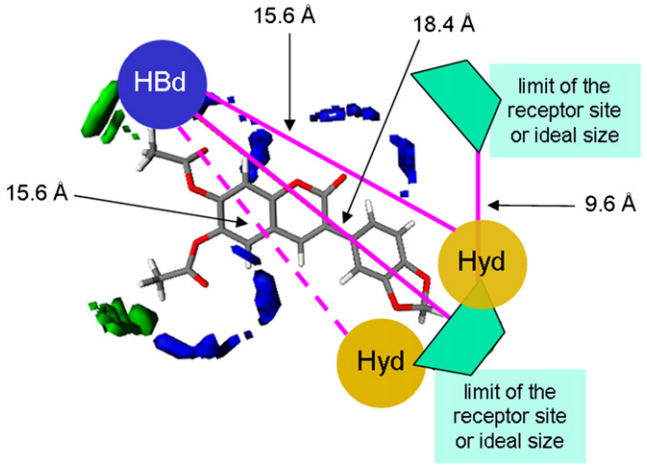

Fig. 8. Resulting pharmacophore for 3-phenylcoumarin derivatives that are biologically active. The depicted molecule (**6**) is one of the most active compounds of the series. The coloured areas around the molecule represent the groups of the virtual receptor site (VRS): HBd, hydrogen bond donor; Hyd, hydrophobic. The green trapezium represents the limits of the VRS (For interpretation of the references to colour in this figure legend, the reader is referred to the web version of this article).

were not known with accuracy; on the other hand, quercetin was not included because it is a chroman-4-one, whilst the other compounds are all chroman-2-ones. Table 3 shows the compounds arranged according to decreasing CL-luc.

Table 3
Structure, parameter values and chemiluminescence[a] for compounds

Compound	$\sigma_I R_6$	$\sigma_I R_7$	$\sigma_I R_{2'}$	$\sigma_I R_{3'}$	$\pi R_{3'}$	$\sigma_I R_{4'}$	$p\mathrm{IC}_{50}$[b] CL-luc	$p\mathrm{IC}_{50}$[c] CL-lum
20	0.33[d]	0.33[d]	0.00	0.33[d]	−0.64[e]	0.33[d]	6.44	6.41
6	0.33[d]	0.33[d]	0.00	0.27[f]	−0.02[e]	0.27[f]	6.16	6.18
5	0.29[d]	0.29[d]	0.00	0.27[f]	−0.64[e]	0.27[f]	6.14	6.14
18	0.33[d]	0.00	0.00	0.33[d]	−0.64[e]	0.33[d]	5.75	5.69
15	0.29[d]	0.00	0.29[d]	0.00	0.00	0.00	5.60	5.55
16	0.33[d]	0.00	0.33[d]	0.00	0.00	0.00	5.59	5.54
14	0.33[d]	0.00	0.00	0.00	0.00	0.33[d]	5.40	4.56
13	0.29[d]	0.00	0.00	0.00	0.00	0.29[d]	5.36	4.53
17	0.29[d]	0.00	0.00	0.29[d]	−0.67[e]	0.29[d]	5.35	5.31
11	0.29[d]	0.00	0.00	0.29[d]	−0.67[e]	0.00	5.28	—[g]
19	0.29[d]	0.29[d]	0.00	0.29[d]	−0.67[e]	0.29[d]	5.28	4.87
2	0.33[d]	0.00	0.00	0.27[f]	−0.02[e]	0.27[f]	5.27	—[g]
1	0.29[d]	0.00	0.00	0.27[f]	−0.02[e]	0.27[f]	5.25	—[g]
12	0.33[d]	0.00	0.00	0.33[d]	−0.64[e]	0.00	5.16	4.66
4	0.00	0.33[d]	0.00	0.27[f]	−0.02[e]	0.27[f]	5.14	—[g]
10	0.33[d]	0.00	0.00	0.00	0.00	0.00	5.13	4.51
9	0.29[d]	0.00	0.00	0.00	0.00	0.00	5.10	—[g]
3	0.00	0.29[d]	0.00	0.27[f]	−0.02[e]	0.27[f]	5.07	—[g]
7	0.00	0.00	0.00	0.27[f]	−0.02[e]	0.27[f]	—[g]	—[g]
8	0.00	0.00	0.00	0.00	0.00	0.00	—[g]	—[g]

[a] $p\mathrm{IC}_{50} = -\log \mathrm{IC}_{50}$, bearing in mind that the higher the value of $p\mathrm{IC}_{50}$ the more potent is the compound.
[b] CL-luc: lucigenin-dependent chemiluminescence.
[c] CL-lum: luminol-dependent chemiluminescence.
[d] See Ref. [29].
[e] See Ref. [31].
[f] See Ref. [30].
[g] It cannot be accurately calculated because $\mathrm{IC}_{50} > 50$ μM.

When compound **19** was not included in deriving Eq. (1) (because there was a great difference between the experimental and theoretical $p\mathrm{IC}_{50}$ values), the result was Eq. (3):

$$p\mathrm{IC}_{50\ \text{CL-luc}} = 4.07 + 3.35(\pm 0.37)\sigma_I R_6 + 2.45(\pm 0.30)\sigma_I R_7 + 1.54(\pm 0.40)\sigma_I R_{2'} + 0.28(\pm 0.29)\sigma_I R_{3'} + 0.82(\pm 0.29)\sigma_I R_{4'}$$
$$n = 17,\ s = 0.134,\ r^2 = 0.927,\ F_{5,11} = 28.28,\ \alpha < 0.001 \quad (3)$$

On the other hand, Eq. (4) resulted when compound **19** was not considered in Eq. (2):

$$p\mathrm{IC}_{50\ \text{CL-luc}} = 4.12 + 3.05(\pm 0.30)\sigma_I R_6 + 2.42(\pm 0.22)\sigma_I R_7 + 1.67(\pm 0.29)\sigma_I R_{2'} + 0.43(\pm 0.13)\pi^2 R_{3'} + 0.91(\pm 0.22)\sigma_I R_{4'}$$
$$n = 17,\ s = 0.101,\ r^2 = 0.959,\ F_{5,11} = 51.80,\ \alpha < 0.001 \quad (4)$$

Interestingly, Eq. (4) showed an inverted parabola in relation to the substituent constant π: the coefficient with the π^2 term is positive. That is, as lipophilicity increased, activity first decreased to a minimum and then increased with further increment in the calculated π. Similar inverted parabolas have been associated with allosteric interactions for enzymes and receptors [35,36].

Much information can be derived from Eqs. (3) and (4); Eq. (4) was slightly better than correlation (3) regarding s, r and F. The probability level is invariably 0.05 for QSAR [37]. The number of degrees of freedom (DF) is $(n - m)$, where n is the number of sets of data (17 in our case) and m is the number of variables [5 in Eq. (4)]. DF is therefore 12, which gives a Student's t value of 2.179 for a probability of 0.05 [32]. The t value was less than the ratio 0.43/0.13, which is the term confidence obtained by dividing the coefficient by its standard error. Therefore, it indicated that the term in π^2 is significant. The same test rejected the $\sigma_I R_{3'}$ term in Eq. (3).

The predictive ability of the models was assessed on the 17 compounds in the training set using the cross-validation approach and measured in terms of a q^2 values. Eq. (4) gave a good q^2 value of 0.958. A model is considered significant when $q^2 > 0.3$ [38]. Regarding the CL-lum and following the same strategy explained for the CL-luc, the following equations were found after removing compound **19** due to the above-mentioned reasons:

$$p\mathrm{IC}_{50\ \text{CL-lum}} = 3.53 + 2.48(\pm 4.65)\sigma_I R_6 + 3.70(\pm 0.67)\sigma_I R_7 + 4.00(\pm 0.98)\sigma_I R_{2'} + 1.26(\pm 0.46)\pi^2 R_{3'} + 1.45(\pm 0.80)\sigma_I R_{4'}$$
$$n = 11,\ s = 0.283,\ r^2 = 0.922,\ F_{4,5} = 11.74,\ \alpha < 0.01 \quad (5)$$

The term $2.48(\pm 4.65)\sigma_I R_6$ was not significant and, when the influence of the R_6 group was considered to be hydrophobic (through π, and π^2), the corresponding correlations did not improve the statistics of Eq. (5); therefore, after removing

the influence of the R_6 group, the relationship (6) was obtained:

$$pIC_{50\ CL\text{-}lum} = 4.34 + 3.74(\pm 0.66)\sigma_I R_7 + 3.88(\pm 0.89)\sigma_I R_{2'} + 1.22(\pm 0.43)\pi^2 R_{3'} + 1.35(\pm 0.73)\sigma_I R_{4'}$$
$$n = 11,\ s = 0.265,\ r^2 = 0.917,\ F_{4,6} = 16.58,\ \alpha < 0.005 \quad (6)$$

The success of QSAR predictions is highly dependent on the number of results from which they are derived, the greater the number, the more reliable the correlation. Four to five biological results for every variable on the right-hand side of the correlation equation is generally regarded as a minimum acceptable level, and the more this figure is exceeded, the better [39]. For this reason, Eq. (6) that takes into account the CL-lum is worse than Eq. (4), which is related to the CL-luc. On comparing Eqs. (5) and (6) the larger coefficient of the term $\pi^2 R_{3'}$ in Eq. (6) than in Eq. (5) draws the attention, and the following hypothesis could be stated: the influence of the hydrophobic interactions is much more important to the CL-lum than to the corresponding CL-luc.

3. Conclusions

In summary, the modulatory action of the investigated 3-phenylcoumarins on IC-mediated neutrophil effector functions seems to require specific structural features, with regard to the number and position of hydroxyl and acetoxyl groups. The structure–activity relationships discussed in this report allowed the identification of new and relevant structural features for selective modulation of the different steps of activation in neutrophil oxidative metabolism, the initial one involving $O_2^{\bullet -}$ generation (measured by CL-luc) or the subsequent involving myeloperoxidase participation (measured by CL-lum).

Although the data set was not very large, we have built a 3D-QSAR model with high statistical significance, which allowed us to propose a virtual receptor site considering both qualitative (pharmacophoric regions) and quantitative aspects (mutual distances). GRIND has shown a high ability to explain the relationships between the structural features of the 3-phenylcoumarin derivatives and their biological activity, independent of but not invariant to the conformations input of the ligands, which was decisive to suggest the possible orientations of the ligands inside the virtual receptor site. The resulting MIF-based pharmacophore suggested the importance of both hydrophobic and hydrogen bond acceptor groups inversely at C-7 and C-3 positions, and also indicated the ideal size of the ligand.

The 2D-QSAR results provided a better correlation for the CL-luc than for the CL-lum. The influence of R_6, R_7, $R_{2'}$ and $R_{4'}$ was inductive, whilst that of $R_{3'}$ was hydrophobic through the substituent constant squared in the CL-luc. Although the effects of the R_7, $R_{2'}$, $R_{3'}$, and $R_{4'}$ groups for the CL-lum were similar to these moieties for the CL-luc, the hydrophobic contribution for the former was much more important, whilst the R_6 substituent did not contribute, either electronically or hydrophobically, to the CL-lum.

Furthermore, since formation and release of different ROS by neutrophils is involved in the development of chronic inflammatory diseases, mediated or not by ICs, the present study could contribute to the development of new molecules to control inflammation and free radical-mediated tissue injury.

4. Experimental

4.1. Chemicals

The 3-phenylcoumarin derivatives were synthesized and characterized as previously described [18,19] (Fig. 1). Lucigenin (bis-*N*-methylacrilidinium nitrate), luminol (5-amino-2,3-dihydro-1,4-phthalazinedione), quercetin (3′,4′,3,5,7-pentahydroxyflavone), ovalbumin and Trypan Blue were purchased from Sigma Chemical Co. (St. Louis, MO, USA). Dimethylsulfoxide (DMSO; Hohenbrunn, Germany), gelatin (Difco Laboratories, Detroit, MN, USA), Triton X-100 (Union Carbide, Houston, TX, USA) and LDH Liquiform (Labtest Diagnostica; Lagoa Santa, MG, Brazil) were the other chemicals used.

4.2. Animals

Adult female New Zealand white rabbits (weight around 3 kg) were used for blood collection and *anti*-ovalbumin antibody production. Animals were handled according to the instructions of The Laboratory Animal Care and Use Ethics Committee from the University of São Paulo, Campus of Ribeirão Preto (Ribeirão Preto, SP, Brazil) and the experimental procedures were approved under protocol number 05.1.1050.53.9.

4.3. Isolation of neutrophils

Blood was collected from the central artery in rabbit's ear into Alsever solution (v/v) as anticoagulant and neutrophils were isolated by the method of Lucisano and Mantovani [40]. Cell pellets were suspended in Hank′s balanced salt solution pH 7.2 (HBSS) containing 0.1% (w/v) gelatin. Cell preparations contained 80–90% neutrophils and viability higher than 95% as established by exclusion with Trypan Blue.

4.4. Preparation of immune complexes

Immune complexes (ICs) were prepared by mixing ovalbumin and polyclonal rabbit *anti*-ovalbumin IgG at equivalence, as determined on the basis of quantitative precipitin curves [41,42]. ICs were then washed twice with cold 0.15 M NaCl (12,000 g, 15 min, 4 °C), and suspended in the same medium. Total protein concentration in the precipitates was determined by absorbance readings at 280 nm and expressed as μg/mL. ICs were diluted in HBSS pH 7.2 for use.

4.5. Cellular chemiluminescence assay

The assay was performed according to Lucisano-Valim et al. [43]. Concentration of each component in the reaction medium (0.8 mL) is indicated in parentheses below. Lucigenin, luminol, quercetin and 3-phenylcoumarins stock solutions were prepared in DMSO. The chemiluminescence probe [lucigenin (0.15 mM) or luminol (0.28 mM)] and test-compound solutions (0–50 μM) or DMSO (control) were added to neutrophil suspensions (1×10^6 cells/mL) and the reaction mixture incubated for 3 min at 37 °C. After addition of IC (60 μg/mL), the reaction tubes were carefully transferred to the luminometer measuring chamber (Autolumat LB953, EG&G Berthold, Germany). The luminol- or lucigenin-enhanced chemiluminescence (CL-lum and CL-luc, respectively) was measured during 30 min at 37 °C. The integrated areas of CL-luc or CL-lum were determined and used to calculate the inhibition percentage promoted by each concentration of the compound tested. IC_{50} values were used to compare their relative activities.

4.6. Cytotoxicity evaluation

Cytotoxic effects of 3-phenylcoumarins on neutrophils were evaluated as described by Lucisano-Valim et al [43]. Briefly, aliquots of cell suspension (10^6 cells/mL) were incubated for 30 min at 37 °C, in the presence of 3-phenylcoumarin solutions (50 μM) or DMSO (control). After centrifugation, cell pellets were immediately suspended in HBSS and cellular viability estimated by the Trypan Blue exclusion test, based on counts of 100 cells. The activity of cytosolic lactate dehydrogenase released into the supernatant was calculated after measuring the decrease of absorbance at 340 nm at 37 °C (Beckman DU-70 spectrophotometer). The LDH Liquiform Kit was used for these measurements. Total cell lysis (positive control) was achieved with 0.2% (v/v) Triton X-100.

4.7. 3D-QSAR procedures

Grid-independent descriptors (GRIND) were generated, analyzed and interpreted using ALMOND 3.3 [27], as implemented in the SYBYL 7.3 package [44]. For a data set containing 13 compounds 570 descriptors have been obtained, using 4 GRID probes: DRY (which represent hydrophobic interactions), O (sp^2 carbonyl oxygen, representing H-bond acceptor), N1 (neutral flat NH, like in amide, H-bond donor), and the TIP probe (molecular shape descriptor). The grid spacing was set to 0.5 Å and the smoothing window to 0.8. The number of filtered nodes was set to 100, with 35% relative weights.

4.8. 2D-QSAR procedures

Statistical analysis of the relationships between CL-luc and substituent properties was performed by the partial least-squares algorithm using the QSAR module of SYBYL 7.3 package [44].

4.9. Modelling of the 3D structures

Three-dimensional structures of the 13 compounds investigated by QSAR were first generated and minimized in Spartan 06 [45], using MMFF force field parameterized in gas-phase. A subsequent conformational search was performed using the MONTE CARLO method with the MMFF molecular mechanics model. The resulting structures were then fully optimized at B3LYP/6-31G* level of calculation.

Acknowledgements

The authors thank Mr. Alcides Silva Pereira and Mrs. Nadir Mazzucato (Faculdade de Ciências Farmacêuticas de Ribeirão Preto, Universidade de São Paulo, Ribeirão Preto-SP, Brazil) for helpful technical assistance, and the Brazilian agencies Conselho Nacional de Desenvolvimento Científico e Tecnológico (CNPq, grant 140462/2003-1), Fundação de Amparo à Pesquisa do Estado de São Paulo (FAPESP, grants 02/06800-4 and 98/14107-0), and Coordenação de Aperfeiçoamento de Pessoal de Nível Superior (CAPES) for financial support.

References

[1] J.A. Schifferli, R.P. Taylor, Kidney Int. 35 (1989) 993–1003.
[2] S. Jancar, M.S. Crespo, Trends Immunol. 26 (2005) 48–55.
[3] B.M. Babior, Am. J. Med. 109 (2000) 33–44.
[4] K.J.A. Davies, IUBMB Life 50 (2000) 279–289.
[5] E. Middleton Junior, C. Kandaswami, T.C. Theoharides, Pharmacol. Rev. 52 (2000) 673–751.
[6] L.M. Kabeya, A. Kanashiro, A.E.C.S. Azzolini, F.M. Soriani, J.L.C. Lopes, Y.M. Lucisano-Valim, Res. Commun. Mol. Pathol. Pharmacol. 111 (2002) 103–114.
[7] A. Kanashiro, L.M. Kabeya, A.C.M. Polizello, N.P. Lopes, J.L.C. Lopes, Y.M. Lucisano-Valim, Phytother. Res. 18 (2004) 61–65.
[8] A. Kanashiro, L.M. Kabeya, C.F.F. Grael, C.O. Jordão, A.E.C.S. Azzolini, J.L.C. Lopes, Y.M. Lucisano-Valim, J. Pharm. Pharmacol. 58 (2006) 853–858.
[9] W.-S. Chang, C.-C. Lin, S.-C. Chuang, H.-C. Chiang, Am. J. Chin. Med. 24 (1996) 11–17.
[10] S. Martín-Aragón, J. Benedi, A. Villar, Phytother. Res. 10 (1996) 75–78.
[11] B. Limasset, T. Ojasoo, C. Le Doucen, J.-C. Dore, Planta Med. 65 (1999) 23–29.
[12] O. Vajragupta, P. Boonchoong, Y. Wongkrajang, Bioorg. Med. Chem. 8 (2000) 2617–2628.
[13] Y.-C. Chen, S.-C. Shen, W.-R. Lee, W.-C. Hou, L.-L. Yang, T.J.F. Lee, J. Cell Biochem. 82 (2001) 537–548.
[14] A. Kumar, B.K. Singh, R. Tyagi, S.K. Jain, S.K. Sharma, A.K. Prasad, H.G. Raj, R.C. Rastogi, A.C. Watterson, V.S. Parmar, Bioorg. Med. Chem. 13 (2005) 4300–4305.
[15] P. McCue, K. Shetty, Crit. Rev. Food Sci. Nutr. 44 (2004) 361–367.
[16] C.M.O. Simões, E.P. Schenkel, G. Gosmann, J.C.P. de Mello, L.A. Mentz, P.R. Petrovick, Farmacognosia: da planta ao medicamento, fifth ed. Editora da UFRGS/Editora da UFSC, Porto Alegre/Florianópolis, 2004.
[17] A.K. Waffo, G.A. Azebaze, A.E. Nkengfack, Z.T. Fomum, M. Meyer, B. Bodo, F.R. Van Heerden, Phytochemistry 53 (2000) 981–985.
[18] A.A. de Marchi, M.S. Castilho, P.G.B. Nascimento, F.C. Archanjo, G. Del Ponte, G. Oliva, M.T. Pupo, Bioorg. Med. Chem. 12 (2004) 4823–4833.
[19] L.M. Kabeya, A.A. de Marchi, A. Kanashiro, N.P. Lopes, C.H.T.P. da Silva, M.T. Pupo, Y.M. Lucisano-Valim, Bioorg. Med. Chem. 15 (2007) 1516–1524.

[20] A.N. García-Argáez, T.O.R. Apan, H.P. Delgado, H. Velázquez, M. Mártinez-Vázquez, Planta Med. 66 (2000) 279–281.
[21] M. Ghate, D. Manohar, V. Kulkarni, R. Shobha, S.Y. Kattimani, Eur. J. Med. Chem. 38 (2003) 297–302.
[22] C.A. Kontogiorgis, D.J. Hadjipavlou-Litina, J. Med. Chem. 48 (2005) 6400–6408.
[23] K. Van Dyke, V. Castranova, Cellular Chemiluminescence, CRC Press, Boca Raton, 1987.
[24] F. Ursini, M. Maiorino, P. Morazzoni, A. Roveri, G. Pifferi, Free Radic. Biol. Med. 16 (1994) 547–553.
[25] M. Payá, M.L. Ferrándiz, F. Miralles, C. Montesinos, A. Ubeda, M.J. Alcaraz, Arzneimittel Forschung – Drug Res. 43 (1993) 655–658.
[26] M. Payá, P.A. Goodwin, B. Heras, J.R.S. Hoult, Biochem. Pharmacol. 48 (1994) 445–451.
[27] M. Pastor, G. Cruciani, I. McLay, S. Pickett, S. Clementi, J. Med. Chem. 43 (2000) 3233–3243.
[28] F. Fontaine, M. Pastor, H. Gutierrez-de-Terán, J.J. Lozano, F. Sanz, Mol. Divers. 6 (2003) 135–147.
[29] R.W. Taft, E. Price, I.R. Fox, I.C. Lewis, K.K. Andersen, G.T. Davis, J. Am. Chem. Soc. 85 (1963) 3146–3156.
[30] S.K. Dayal, S. Ehrenson, R.W. Taft, J. Am. Chem. Soc. 94 (1972) 9113–9122.
[31] D.H. McDaniel, H.C. Brown, J. Org. Chem. 23 (1958) 420–427.
[32] J.M. Blaney, C. Hansch, in: C. Hansch, P.G. Sammes, J.B. Taylor (Eds.), Comprehensive Medicinal Chemistry. vol. 4. The Rational Design, Mechanistic Study and Therapeutic Application of Chemical Compounds, Pergamon Press, Oxford, 1990, pp. 459–496.
[33] C. Hansch, J.M. Blaney, in: J.K. Seydel, K.-J. Schaper (Eds.), Chemische Struktur und biologische Aktivität von Wirkstoffen. Methoden der Quantitativen Struckutr-Wirkung-Analyse, Verlag Chemie, Weinheim, 1979, pp. 185–208.
[34] C. Hansch, R. Garg, A. Kurup, Bioorg. Med. Chem. 9 (2001) 283–289.
[35] R. Garg, A. Kurup, S.B. Mekapati, C. Hansch, Bioorg. Med. Chem. 11 (2003) 621–628.
[36] H.J. Smith (Ed.), Smith and Williams' Introduction to the Principles of Drug Design, second ed. John Wright, London, 1988.
[37] L. Sachs, Applied Statistics. A Handbook of Techniques, second ed. Springer-Verlag, New York, 1984.
[38] C.G. Wermuth, The Practice of Medicinal Chemistry, second ed. Elsevier Academic Press, London, 2003.
[39] F.D. King, Medicinal Chemistry. Principles and Practice, The Royal Society of Chemistry, Cambridge, 1994.
[40] Y.M. Lucisano, B. Mantovani, J. Immunol. 132 (1984) 2015–2020.
[41] J.L. Fahey, J. Wunderlich, R. Mishell, J. Exp. Med. 120 (1964) 223.
[42] E.A. Kabat, M.M. Mayer, Experimental Immunochemistry, second ed. Thomas, Springfield, 1961.
[43] Y.M. Lucisano-Valim, L.M. Kabeya, A. Kanashiro, E.M.S. Russo-Carbolante, A.C.M. Polizello, A.E.C.S. Azzolini, S.C. Silva, J.L.C. Lopes, C.A. Oliveira, B. Mantovani, J. Pharmacol. Toxicol. Methods 47 (2002) 53–58.
[44] SYBYL 7.3, Tripos, Inc., USA, 2006.
[45] Spartan '06 full, Tutorial and User's Guide, Wavefunction, Inc., USA, 2006.